XVII IMEKO World Congress
Metrology in the 3rd Millennium
June 22−27, 2003, Dubrovnik, Croatia

A PARAMETRIC MODEL FOR THE UNCERTAINTY OF DIGITAL IMAGES

Consolatina Liguori[(1)], *Alfredo Paolillo*[(2)], *Antonio Pietrosanto*[(2)]

[(1)]DAEIMI, University of Cassino, Cassino (FR), Italy
[(2)]DIIIE, University of Salerno, Fisciano (SA), Italy

Abstract – In this paper a parametric model of the uncertainty of digital images in industrial contest is presented and characterized. The functional dependency of the model parameters from the operating conditions and the image characteristics are theoretically established and experimentally verified.

Keywords – Image based measurements, uncertainty, digital image

1. INTRODUCTION

The use of digital images is getting widespread in several fields of engineering. This diffusion is due to noticeable progresses made in the field of image processing both by dedicated hardware technologies (processors, cameras, frame grabbers) and by software products (image encoders, edge detectors, etc…). Automatic measurement systems based on digital image processing are today proposed and used in several industrial applications where contact-less measurements of geometrical parameters are needed for process or quality control. Area, length, width measurement can be provided by these systems without requiring that the object under measurement be moved or touched by the measurement system.

In ISO 9000 certified environments, however, image based measurements, such as every other measurement, must be completed by a quantitative indication of quality. The Guide to the expression of Uncertainty in Measurement (GUM) [1] standardizes the measurement quality expression, defining the uncertainty as “a parameter, associated with the result of a measurement, that characterizes the dispersion of the values that could reasonably be attributed to the measurand”. The uncertainty, u, completely describes the measurement reliability if the result is corrected for all known systematic effects (bias) that significantly influence the estimation. In other hands, each time a measurement process has to be characterized both systematic and random error effects must be estimated in order to qualify the obtained results with the standard uncertainty. As far as the image processing based measurements are concerned, these effects depend on the characteristics of the digital device, on the measured object and its background, on some external parameters that may influence the image acquisition, and, finally, on the image processing algorithms [2]-[4].

The u of measurement results can be experimentally evaluated by statistical methods (type A evaluation). At first, deterministic errors must be estimated through a comparison to a reference object or instrument that will provide a correction with its uncertainty, u_c. The standard deviation of results, s_r, is then evaluated in a set of measurements carried out when both the measurand and all the controllable influence parameters are kept constant. The standard uncertainty of the corrected measurements, u, is finally equal to the square root of $u_c^2 + s_r^2$.

In spite of its attractiveness, this immediate (black box) approach to the evaluation of u is worthwhile only when test conditions are limited to few configurations and the measurand can be easily kept constant during the image acquisitions. Otherwise, since a complete characterization requires that all the external influence factors (vibrations, lights, background), internal measurement parameters (focus, shutter and so on), and options of the image processing software be held into account, a combinatorial explosion of the number of tests would be possible. Furthermore, whenever the measurand itself exhibits uncontrollable variability, an accurate type A estimate of u cannot in any case be carried out.

In alternative, if an analytical expression of the image intensity uncertainty due to the influence of external and internal factors on the digitalization process were available, the measurement result uncertainty could be computed (Type B evaluation) by applying the Uncertainty Propagation Law [1] to the image processing algorithm. This “predictive” type B evaluation would not require that suitable tests be carried out, and could be useful even in driving the measurement system design.

Looking toward this aim, the authors proposed a typical white box approach to the metrological characterization of image processing based measurement systems [5]. As first step, the authors tackled the problem of defining a parametric model of the digital image intensity uncertainty. A parametric relationship between the standard deviation of the pixels intensity I(i,j) and the characteristics of the neighborough was found [5]. Even if matching with experimental results, this relationship does not allow the standard uncertainty of I(i,j) to be evaluated, because both the deterministic errors and the dependence of the expression parameters on the external influence factors are not yet analytically defined. In this paper, a complete analysis of systematic effects and an experimental study of the dependence of the parameters on the main external influence factors is made. At first, a method for the evaluation and correction of systematic effects is described and applied. Then, after a brief recall on the parametric model, all the experimental tests carried out to determine the influence of flicker and vibrations on the model parameters are presented and commented. Finally, the whole method is applied to some real cases with the aim of analyzing both the robustness and the accuracy of the model.

2. METROLOGICAL CHARACTERIZATION OF A DIGITAL IMAGE

The image acquisition process is affected by systematic and random events. As a consequence, in order to characterize a digital image both systematic errors and random variability must be estimated. In particular, the systematic errors arising from recognized effects of influence quantities have to be quantified and the correction has to be applied. Then the uncertainty of the corrected image, that defines for each pixel an intensity value interval that contains the expected intensity value, can be evaluated.

2.1 Systematic effects and correction

The most common device used to produce digitized images from the real world is the CCD (Charge Coupled Device). Generally, this device gives, for each pixel, a quantized level proportional to the number of photons that hit the sensing area of that pixel during a given exposure time. Several causes of noise are known for CCDs [6]. Some of them give rise to differences in the response of different pixels not depending on the photon flux, that remain constant during time. Another unwanted effect is the (spatial) non-uniformity of the response of each pixel to the photon flux. Generally, the image acquisition with a CCD can be modeled, for each pixel (i,j), as [7]:

$$I_{ACQ}(i,j) = I_D(i,j) + r(i,j)I_o(i,j) \tag{1}$$

where:

$I_{ACQ}(i,j)$ is the acquired digital image;

$I_D(i,j)$ is called the *dark frame* because it is acquired in total absence of light. It takes into account, for each pixel, the systematic component of the CCD noise. It has to be evaluated and subtracted from the acquired image:

$$I_C(i,j) = I_{ACQ}(i,j) - I_D(i,j) = r(i,j)\cdot I_0(i,j) \tag{2}$$

However, the error correction can be avoided whenever it results negligible with respect to uncertainty of the digital image $u_{I_{ACQ}}(i,j)$;

$r(i,j)$ called the response matrix, models the non-uniformity of the response of the pixel (i,j) to the light. It holds into account both the possible imperfections of the CCD itself, and dust and halos that could be present on the CCD or lens surfaces;

$I_o(i,j)$ is the expected image, due only to the number of photons that hit the pixel area.

From relationship (1) the expected image can be calculated as: $I_o(i,j) = \frac{I_C(i,j)}{r(i,j)} = \frac{I_{ACQ}(i,j) - I_D(i,j)}{r(i,j)}$ (3).

2.2 Random effects

Random variability of the pixel intensity is due to both internal and external influence parameters. Influence quantities are attained by the general knowledge of the acquisition system and of the working environment. Significant parameters can also be associated with the illumination conditions of the object (power and position of the light sources) flicker, and so on. All of them generate a random variability of the acquired pixel intensity. This variability can be quantified, for each pixel, as the standard deviation of its intensity, and can be reported in form of uncertainty matrix $u_{I_{ACQ}}(i,j)$.

2.3 Uncertainty of the expected image

Once the corrections of systematic effects have been applied, and the uncertainty on the acquired image is estimated, the standard uncertainty of the expected image I_0 can be evaluated. In particular, applying the uncertainty propagation law to (3) a direct relationship is obtained:

$$\begin{aligned} u^2_{I_o}(i,j) &= \left[\frac{I_{ACQ}(i,j) - \bar{I}_D(i,j)}{r^2(i,j)}\right]^2 u_r^2(i,j) + \\ &+ \frac{1}{r^2(i,j)} u^2_{I_D}(i,j) + \frac{1}{r^2(i,j)} u^2_{I_{ACQ}}(i,j) \end{aligned} \tag{4}$$

Where $u_r(i,j)$, $u_{I_D}(i,j)$ represent the uncertainty on the response matrix and on the estimated dark frame, respectively. It is evident that if a correction of systematic errors is made, also the uncertainty of the correction contributes to the final uncertainty; but even if the error correction increases the uncertainty, corrected mean values are closer to expected values than uncorrected ones.

3. SYSTEMATIC ERRORS IN DIGITIZING IMAGES: EVALUATION AND CORRECTION

Dark frame and response matrix represent systematic effects which strictly depend on the image acquisition hardware (lens, CCD sensor) and on its operative conditions (iris, shutter, focus). These characteristics can be considered as invariant parameters for most of the industrial applications. As a result, the required *una tantum* evaluation of both the $I_D(i,j)$ and $r(i,j)$ is worth being experimentally made.

The experimental procedure for the systematic effects evaluation can be better explained with reference to a specific hardware, in the case a CCD camera JAI CV-A50 with optics having focal length f = 25mm and F number = 1.4, with 256 grey level and 566x758 pixels; with a stabilized and floating supply that allows a better normal mode noise rejection.

3.1 Dark frame

The evaluation of the dark frame can be done experimentally, by averaging pixel by pixel a sample of N images $\{I_D(i,j)\}$ acquired while the CCD is not being exposed to any incident light. This average image $\bar{I}_D(i,j)$ is then subtracted from the acquired image (see equation (2)).

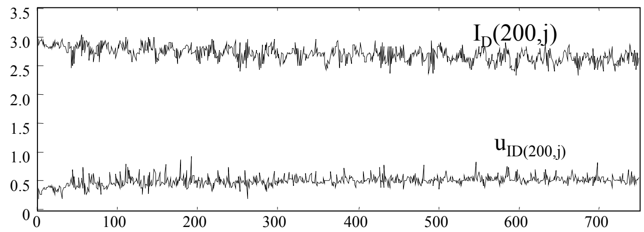

Fig.1 A row of the averaged dark frame and its standard uncertainty.

The standard uncertainty of $\bar{I}_D(i,j)$ can be posed equal to the standard deviation, pixel by pixel, of the sample of the N images, $u^2_{\bar{I}_D}(i,j) = \sigma^2\{I_D(i,j)\}/\sqrt{N}$. Fig.1 shows a row of a matrix $\bar{I}_D(i,j)$ and its uncertainty, evaluated on N=30 images. In this example, the values of the dark frame fall in the range [2.5, 3.0]. When the spatial variability of the dark frame is low it can be approximated by a constant matrix.

It has to be noted that camera models are present on the market that allow to automatically subtract a fixed gray level value ("black level"), thus obtaining a result approximately similar to the application of the dark frame correction; obviously this process should be taken into account in the uncertainty estimation.

3.2 Response matrix

A second issue has to be considered now, given that the response r(i,j) of the pixel is, in general, different for each pixel. After the application of (3), the equation (2) becomes:

$$I_C(i,j) = r(i,j) I_o(i,j) \tag{5}$$

Also the matrix r(i,j) can be experimentally determined, acquiring a sample of N images $\{I_{FF}(i,j)\}$ of a surface uniformly lit: in this condition, the number of photons hitting each pixel is the same. In particular, the pixel-by-pixel average $\bar{I}_{FF}(i,j)$ of these images, called the *flat field*, is considered. It is worth noting that the dark frame has to be subtracted from this image, too, and here in after the flat field will be supposed already corrected for systematic effects. Furthermore, the mean spatial value of the intensity of the pixel of this image is computed:

$$I_{FF,Mean} = \frac{1}{N_{row} \times N_{col}} \sum_{i=0}^{N_{row}-1} \sum_{j=0}^{N_{col}-1} \bar{I}_{FF}(i,j) \tag{6}$$

The response of each pixel can be written as:

$$r(i,j) = \frac{\bar{I}_{FF}(i,j)}{I_{FF,Mean}} \tag{7}$$

where the term $I_{FF,Mean}$ can be considered as the wanted, spatially-constant, value of the response, while $\bar{I}_{FF}(i,j)$ is its actual "non-uniform" value when the scene is a surface uniformly lit. The uncertainty of $\bar{I}_{FF}(i,j)$ is evaluated as the measured standard deviation: $u^2_{\bar{I}_{FF}}(i,j) = \sigma^2\{I_{FF}(i,j)\}/\sqrt{N}$

while the uncertainty of $I_{FF,,Mean}$, is derived from (6) as:

$$u^2_{I_{FF,Mean}} = \frac{1}{N_{row} \times N_{col}} \sum_{i=0}^{N_{row}-1} \sum_{j=0}^{N_{col}-1} u^2_{\bar{I}_{FF}}(i,j) \tag{8}$$

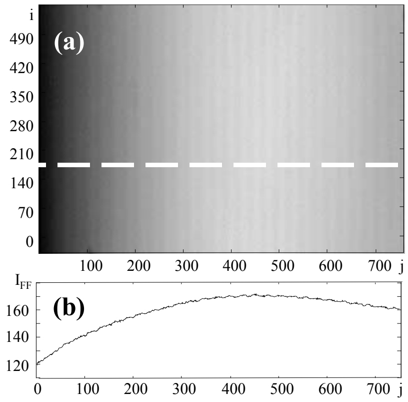

Fig.2 The whole averaged flat field (a) and a single row (b).

In order to evaluate the uncertainty of r(i,j) the uncertainty propagation law is applied to (7); and considering the correlation with easy calculations we have:

$$\dot{u}^2_r(i,j) = \dot{u}^2_{\bar{I}_{FF}}(i,j)\left(1 - \frac{2}{N \times M}\frac{\bar{I}_{FF}(i,j)}{I_{FF,Mean}}\right) + \dot{u}^2_{FF,Mean} \cong \dot{u}^2_{\bar{I}_{FF}}(i,j) + \dot{u}^2_{FF,Mean} \tag{9}$$

where the notation $\dot{u}$ states for relative uncertainty.

In some cases, it could be hard to strictly achieve the condition of an equal number of photons hitting each CCD cell. Often, only a good approximation can be realized and several experimental set-ups have been applied in different research areas. In the experimental tests described in this paper, the flat fields were taken by framing a transparent white screen that was being lit by the sun light on the opposite side. In Fig.2 the values of the averaged flat field $\bar{I}_{FF}(i,j)$ are shown together with the value of a single row. As can be seen, the overall response of the pixels belonging to the center of the image is higher than the response in outer regions of the image; furthermore, the response is evidently non-symmetric.

4. UNCERTAINTY OF THE ACQUIRED IMAGE

4.1 Parametric model

As mentioned in the introduction, the experimental evaluation of the $u_{I_{ACQ}}(i,j)$ is not always possible and/or suggested. Furthermore, in some occasions a preventive analytical evaluation of $u_{I_{ACQ}}(i,j)$ can be very useful. These considerations drove the authors to the definition of an analytical model of the image uncertainty. It is expressed in terms of analytical relationship, which yields an estimation of $u_{I_{ACQ}}(i,j)$, say $\hat{u}_{I_{ACQ}}(i,j)$, and takes into account the influence of all the measurement conditions and the image characteristic parameters. It implements the effects of internal influence quantities that are always significant, such as spatial and intensity quantization, as well as the influence of the image characteristics. As far as the external influence quantities are concerned, since their significance is different for different applications and for different working environments, specific approximations were made.

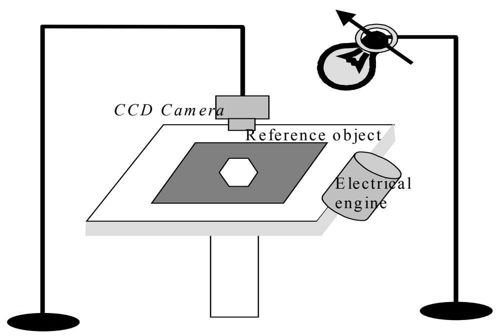

Fig. 3 Some parts of the measurement system

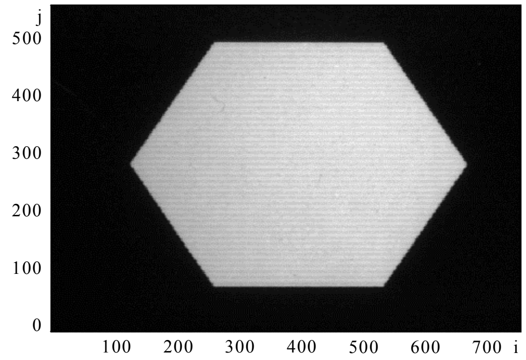

Fig. 4 An image of the reference object

The hypothesized analytical expression of the pixel uncertainty model $\hat{u}_{I(i,j)}$ is the following:

$$\hat{u}^2_{IACQ}(i,j) = K_\Delta \left|\frac{\partial I(i,j)}{\partial i}\right| \cdot \left|\frac{\partial I(i,j)}{\partial j}\right| + K_C \cdot I^2_{ACQ}(i,j) + K_q \quad (10)$$

Where the parameters K_Δ, K_C, K_q, are constant weights depending on specific working conditions characterizing industrial environments.

4.2 Model parameter determination

It is easy to understand that the validity of the aforementioned model is deeply conditioned by the accuracy used to determine the parameters K_Δ, K_C, Kq. A measurement station was properly set up to carry out the tests for the experimental evaluation of the functional relationships among the working conditions and the model parameters.

The measurement station

The measurement station, besides image acquisition and processing equipments, see Fig. 3, include also devices for the monitoring and control of external influence factors. In particular it consist of:

i) An equipment, fixing the distance between the camera and the object.
ii) The same CCD camera used for the test reported in Section 3 (JAI CV-A50).
iii) An unbalanced variable voltage power supplied, whose controlled and measured ibrations can be transmitted to the target object.
iv) An accelerometer Kistler Piezotron 8712A5M1 (5g measuring range), transduces the vibration signal in a voltage signal.
v) An illumination system, based on a set of DC halogen lamps (6V, 20W), whose power supply is fed by the amplified output of a waveform generator, in order to produced amplitude and/or frequency controlled flicker.
vi) A suitably conditioned photodiode gives a voltage output proportional to the incident light power. The voltage/lux conversion factor was obtained by a calibration with a reference lux-meter.
vii) A PC hosting a frame-grabber (National Instruments PCI-1409) and a data acquisition board (National Instruments PCI-MIO-16E-1) for the image and signal acquisition and processig.

The procedure for model parameter estimation

For each working condition, a set of N=30 images of a reference object are acquired. In order to avoid other influence factors, the object is a simple shape drawn on a paper sheet with a uniform color on a background of constant color: a white hexagon on a black background, see Fig.4. For each image set, $(I(i,j)_1,\ldots.I(i,j)_N)$ the uncertainty $u_{I_{ACQ}}(i,j)$ is statistical evaluated: for each pixel, $u_{I_{ACQ}}(i,j)$ is measured as the standard deviation of the intensity I. Then, the best fitting value of the model parameters in equation (10) are determined by minimizing ε, defined as the the distance between the uncertainty estimated by equation (10), $\hat{u}_{I_{ACQ}}(i,j)$, and the measured one $u_{I_{ACQ}}(i,j)$:

$$\varepsilon = \sum_{i=1}^{row}\sum_{j=1}^{col}\left(u_{I_{ACQ}(i,j)} - \sqrt{K_\Delta \left|\frac{\partial I(i,j)}{\partial i}\right| \cdot \left|\frac{\partial I(i,j)}{\partial j}\right| + K_C I^2_{ACQ}(i,j) + K_q}\right)^2 \quad (12)$$

The minimization of this non-linear relationship is performed by a Levenberg-Marqardt optimization algorithm [8], adapted to the specific multidimensional case. The inputs for the minimization procedure are the measured uncertainty $u_{I_{ACQ}}(i,j)$ and one sample image extracted from the acquired set, while its outputs are three optimum values for K_Δ, K_C, K_q. However, for each working condition, the minimization is run N times, using each one of the images in turn as sample image. In this way, a set of N=30 values for each model parameter K is available; the average value is used as the best estimate of the parameter and the standard deviation, σ_{Ki} measured on the set expresses the parameter uncertainty.

Experimental tests

Since the main application area of the proposed model is in industrial environments, the authors' experience [5], [9]-[10] suggested considering as more significant influence factors:

– flicker of light sources, due, for instance, to the instability of the line power supply;
– vibration of the target object due to the industrial process.

The tests were planned in several sessions, each one of them yielding the best set of model parameters, for the following combinations of flicker, vibrations and illumination level:

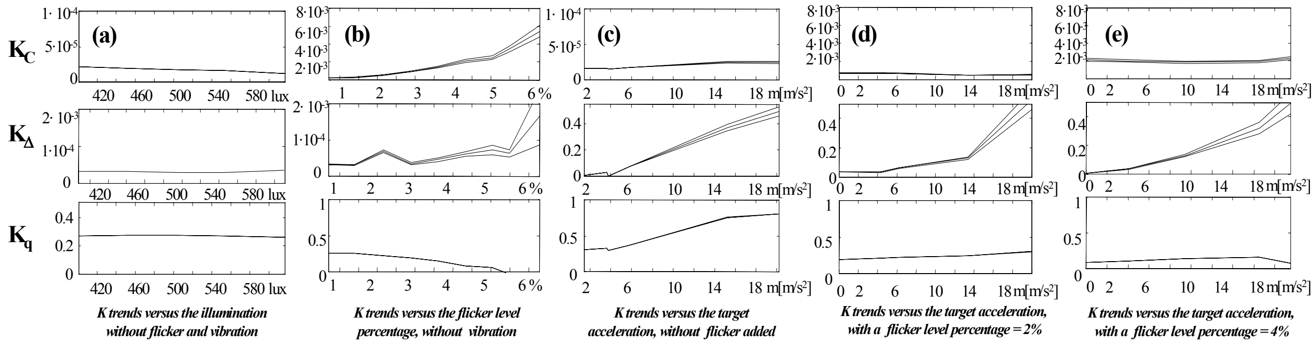

Fig.5 The measured optimum parameter plotted with their uncertainty interval ($K_i \pm \sigma_{Ki}$) versus the influence factors.

a) No flicker, no vibrations, different working conditions are obtained by changing illumination level, see Fig.5(a).
b) No vibrations, constant illumination level, different working conditions are obtained by changing the amplitude flicker level, see Fig. 5 (b). In the figures, in order to indicate the measured flicker level a synthetic parameter is used: L_1/L_{DC}, where L_{DC} is the dc value of the illumination and L_1 the peak-to-peak amplitude of the first harmonic of the ripple, both measured in lux.
c) No flicker, constant illumination level, different working conditions are obtained by changing vibration level, see Fig. 5(c). The vibration level is expressed in terms of rms value (in m/s^2) of the first harmonic of the measured acceleration of the target.
d) Constant illumination different working conditions are characterized by combinations of flicker and vibrations. In particular for two different levels of illumination flicker, L_1/L_{DC} equal to about 2% (Fig.5(d)) and about 4% ((Fig.5(e)), a raising amount of vibration was impressed to the target.

4.3 Model parameters and influence factors

The dependence of the model parameters on the influence quantities can be taken out by analyzing the experimental results, summarized in Fig. 5.

i) The model parameters are not influenced at all by the illumination level.
ii) The model parameter K_C is significantly dependent only on the flicker level, since its variability versus vibrations is negligible.
iii) The model parameter K_Δ is practically insensitive to flicker, while it increases steeply with vibrations.
iv) The parameter K_q depends slightly on both the influence quantities; namely it decreases with the flicker and increases with vibrations.

If the problem of setting up an Image Based Measurement System in a typical industrial environment is considered, the fine-tuning of the model parameters can turn out as a hard task, even if these results were available in graphical or in table form, because it would require accurate measurements of the influence quantities. In this context, a handy solution can be represented by synthetic tables, which give the value of the parameters by entering with very basic and perceivable information about the influence quantity instead of measured values. For instance, one can say whether an object to be measured is lit with a level of flicker null, low or high, which is a subjective, fuzzy but easily achievable kind of information. In Fig. 6, the results obtained following this approach are reported. As can be seen, the parameter values are given with respect to such coarse sets of the influence quantities. In particular, the threshold between "low" flicker and "high" flicker is chosen at about $L_1/L_{DC} = 3\%$, and the threshold between "low" and "high" vibration is chosen at about 0.015 m/s^2 of the rms value of 1st harmonic of the acceleration signal. It has to be underlined that these thresholds have been chosen following a perceptive criterion, and the values are determined as average values within the specific ranges.

5. EXAMPLES

In order to verify the goodness of the approach, several tests were carried out on a flat target object different than the one used for the model parameter estimation. It is composed of some areas at different gray tones, see Fig.7.

For each test the conditions for the flicker and for the vibration were arbitrarily chosen, and a subjective evaluation was made ("null","low" or "high") for the level of the two influence quantities. Then a single image was taken from this scene, and the corresponding parameters of Tables reported in Fig.6 were used in (10) in order to

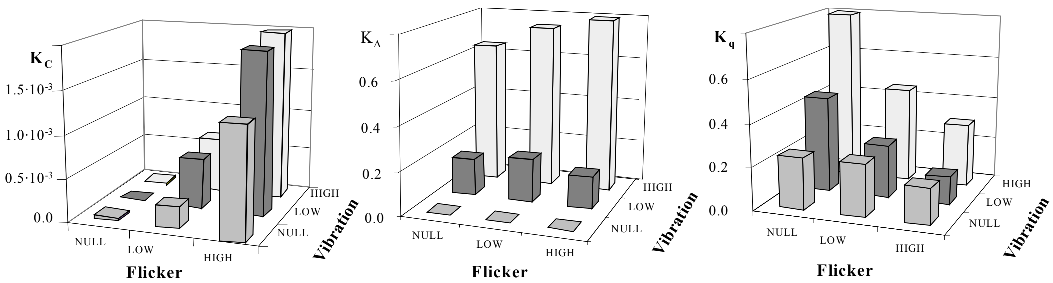

K_c (Vibration \ Flicker)	NULL	MED	HIGH
NULL	$3.2\cdot10^{-5}$	$2.5\cdot10^{-4}$	$1.3\cdot10^{-3}$
LOW	$1.9\cdot10^{-5}$	$6.0\cdot10^{-4}$	$1.9\cdot10^{-3}$
HIGH	$2.5\cdot10^{-5}$	$6.5\cdot10^{-4}$	$2.0\cdot10^{-3}$

K_Δ (Vibration \ Flicker)	NULL	MED	HIGH
NULL	$2.9\cdot10^{-4}$	$4.0\cdot10^{-4}$	$4.0\cdot10^{-4}$
LOW	$1.7\cdot10^{-1}$	$2.0\cdot10^{-1}$	$1.5\cdot10^{-1}$
HIGH	$6.5\cdot10^{-1}$	$7.5\cdot10^{-1}$	$8.0\cdot10^{-1}$

K_q (Vibration \ Flicker)	NULL	MED	HIGH
NULL	0.24	0.24	0.17
LOW	0.45	0.25	0.13
HIGH	0.80	0.45	0.30

Fig. 6 Synthetic values of the model parameters with respect to coarse classes of influence quantities.

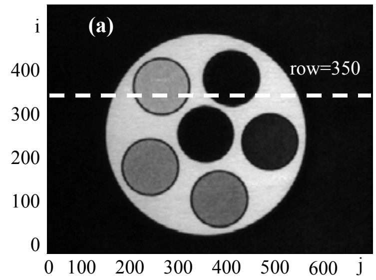

Fig.7 An image of the test object

determine the estimated image uncertainty $\hat{u}_{I_{ACQ}}(i, j)$. Finally, a set of 30 images was taken from the same scene in order to measure uncertainty $u_{I_{ACQ}}(i, j)$. In Fig.8 some plots are reported showing the comparison for the estimated $\hat{u}_{I_{ACQ}}(i, j)$ and the measured $u_{I_{ACQ}}(i, j)$. In the figures the agreement between the two trends is evident, thus confirming goodness of the proposed model and the used parameters.

6. CONCLUSIONS

In the paper the problem of the image-based measurement uncertainty was tackled with reference to both systematic and random effects. Some main causes of deterministic error in the digital image acquisition were analyzed and a correction procedure was defined. A parametric model of the digital image uncertainty was enhanced through the experimental evaluation of the functional dependence of the model parameters (K_c,K_Δ and K_q) on the two principal causes of uncertainty in industrial environments: light flicker and vibrations. The results of the numerous experimental tests carried out on simple and complex shapes show that the uncertainty analytical estimate allowed by the parametric model is very accurate if measurements of light flicker intensity and vibration level can drive the choice of the parametr values. On the other hand, quantitative suggestions for a more practical use of the model in typical industrial environments were experimented in other tests. These results evidence that the accuracy in the prediction of uncertainty is acceptable even if the evaluation of the external factors is “thumb” made. Future developments will concern the extension of the parametric model application field to new categories of objects and backgrounds.

ACKNOWLEDGMENTS

The author wishes to thank Dr. Umberto Berlen and Dr. Domenico Granozio for the help given in the experimental phase.

REFERENCES

[1] BIPM, IEC, IFCC, ISO, IUPAC, IUPAP, OIML, “Guide to the expression of uncertainty in measurement”, 1993.
[2] D.I. Havelock, "Geometric Precision in Noise-Free Digital Images", IEEE Transaction on Pattern Analysis and Machine Intelligence, vol. PAMI-11, n.10, October 1989
[3] B.Kamgar-Parsi and B.Kamgar-Parsi, "Evaluation of Quantization Error in Computer Vision", IEEE Transaction on Pattern Analysis and Machine Intelligence, vol. PAMI-11, n.9, September 1989.
[4] C. Ho, "Precision of Digital Vision Systems", IEEE Transaction on Pattern Analysis and Machine Intelligence, vol. PAMI-5, n.6, November 1983.
[5] M. De Santo, C. Liguori, A. Pietrosanto: “Uncertainty characterization in image-based measurements: a preliminary discussion”, IEEE Transactions on Instrumentation and Measurement, vol. 49, N. 5, October 2000, pp. 1101-1107.
[6] Steve Howell, "Scientific Charge Coupled Devices", Cambridge University Press
[7] James Janesick, "Scientific Charge Coupled Devices", SPIE Press, Vol. PM83, Jan 2001, ISBN 0-8194-3698-4
[8] J.E.Dennis and R.B. Schnabel: Numerical Methods for Unconstrained Optimization and Nonlinear Equations, Prentice-Hall, 1983, SIAM, 1996.
[9] L. Angrisani, P. Daponte, C. Liguori, A. Pietrosanto: “An image-based measurement system for the characterization of automotive gaskets”, Measurement, vol. 25, pp. 169-181, April 1999.
[10] C. Liguori, A. Paolillo, A. Pietrosanto: “An on-line stereo vision system for dimensional measurements on rubber extrusions”, 11th IMEKO TC-4 Symposium, September 2001, Vol. I pp. 25-28

Authors: Prof. Consolatina Liguori, DAEIMI, University of Cassino, via G. Di Biasio 47, 07047, Cassino (FR), Italy, Phone:++39 0776299672, Fax ++39 0776299707 e-mail: liguori@unicas.it. Dr. Alfredo Paolillo, DIIIE, University of Salerno, via ponte Don Melillo, 84084, Fisciano (SA), Italy, Phone ++39 089964248, Fax ++39 089964218, e-mail apaolillo@unisa.it. Prof. Antonio Pietrosanto, DIIIE, University of Salerno, via ponte Don Melillo, 84084, Fisciano (SA), Italy, Phone ++39 089964248, Fax ++39 089964218, e-mail apietrosanto@unisa.

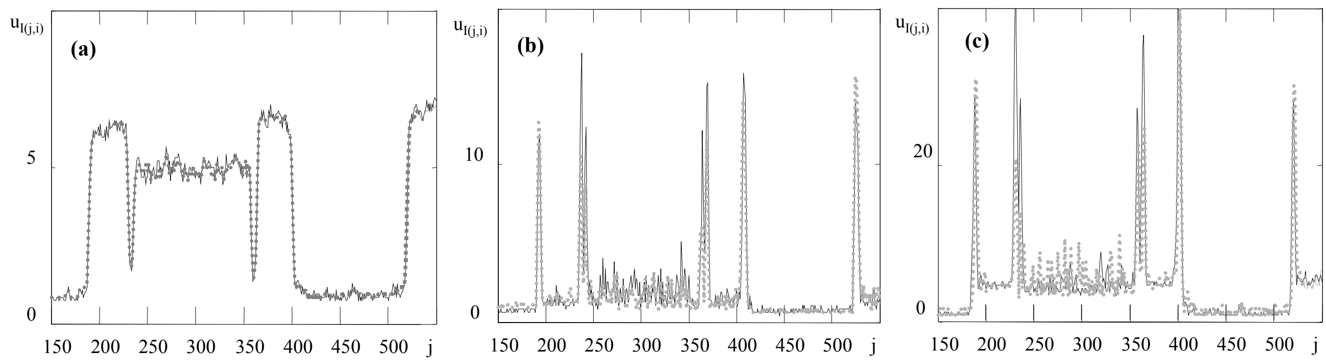

Fig. 8 Comparison between $u_{I_{ACQ}}(i, j)$ (dotted line) and $\hat{u}_{I_{ACQ}}(i, j)$ (solid line) in case of (a) high flicker, b) low vibration, c) low flicker and high vibration